GROUND MOTIONS, IMPLICATIONS FOR BUILDING CODES

by

Neville Donovan

Introduction

In 1969, before memories of the March 27, 1964 Prince William Sound Earthquake (M_s = 8.4) had faded and while the design considerations for the oil pipeline across Alaska were in the planning stages, we were asked to provide seismic design recommendations for the entire pipeline system. From the outset it appeared that some recognition of seismic probability would be a useful way to characterize the requirements for the 1200 kilometer long pipeline route which passes through extensively varied tectonic and geologic conditions and crosses the Denali Fault, one of the most spectacularly expressed seismic faults in the world.

A probabilistic study was undertaken and a detailed report prepared. The probabilistic procedure was able to show that the method and results were in "agreement" with estimates of ground motion in Southern Alaska during 1964. The probabilistic method was also the only procedure able to quantitatively consider multiple occurrences of such events as underwater cable failures caused by submarine landslides in the Valdez area. Valdez is a deep fjord where earthquake-induced submarine landslides in the glacial sediments occur relatively frequently. It was a slide from the glacial delta which destroyed a large part of the town of Valdez in 1964. When the results of this study were presented to the regulatory agency it was not prepared to accept the procedure.

Difficulty in obtaining acceptance of a new procedure is a relatively commonplace happening. Now that probabilistic studies are part of the design process for major construction projects and are also the established basis for the development of seismic zoning maps prepared with active participation of the group which refused to accept our Alaska work, it is often overlooked that this acceptance is a very recent one. Among the countries on the American continent Canada is the only one which has adopted a seismic zoning map based on probabilistic procedures. Although the ATC-3-06 map for the United States was prepared by 1976, over ten years ago, it has yet to be adopted by code groups such as the

International Conference of Building Officials which publishes the Uniform Building Code.

Seismic Hazard Studies

Probabilistic seismic hazard studies require the combined efforts of professionals in many disciplines. For example, the geologist is responsible for defining the regional tectonics and delineating the seismic sources. In some areas where the tectonic patterns are reasonably well understood and the faults well known, global estimates of slip rates can be used to augment seismological data. We are fortunate in San Francisco to have an area on a comparatively straight-forward tectonic plate boundary that has been studied in some detail. This allowed comparative studies between the historical seismology and the recurrence estimates based on global slip rates. Slip rates estimated on the major faults in the system were compared with the total slip obtained by geodetic measurements across the plate boundary. The geodetic slip rate in the San Francisco Bay Area measured by triangulation across the plate boundary between Mt. Diablo and the Farallon Islands is about 6 cm. per year.

As an example, consider how the different sets of input information can be combined by tracing the process used for a recent study in San Francisco. The study area is outlined together with the major faults in Figure 1. The historic seismic record is shown schematically on Figure 2. Early events have been given equivalent magnitudes using the $M = 2/3\ I + 1.0$ relationship of Richter (1958). This conversion relationship produced some clustering of events on the recurrence curve given on Figure 3 because intensity values are only recorded as integers. A least-squares fit to the data for the events shown on Figure 3 gave the following regional seismic recurrence relationship:

$$\log N = 4.93 - 0.614M \qquad (1)$$

where N is the number of events having a magnitude equal to or greater than M within the area defined on Figure 1 during the 132-year period of the historical data set.

Equation (1) defines the activity rate and the magnitude distribution of the activity, which are used in the probability calculations for the seismic risk assessment.

Some recent seismological studies have questioned whether the seismic activity curve developed from the Gutenberg and Richter plot correctly represents the seismic activity, especially with respect to large earthquakes (Youngs and Coppersmith, 1985). Others (Anderson, 1984) have suggested that the slope of a recurrence plot such as that shown on Figure 3 may be a consistent parameter on some faults even where there are relatively long quiescent periods between major events. In this case the filling out of the recurrence curve is accomplished by aftershocks.

Some studies have used global slip rates as a means of placing constraints on recurrence relationship (Molnar, 1979) while others suggest (Joyner and Fumal, 1985) that if the ground motion estimates are consistent with observed slip rates they can be developed independently of assumptions concerning the seismic recurrence relationships shown on Figure 3. Faced with these diverse alternatives it was decided that a check should be made to see whether the total global deformation in the Bay Area is consistent with the historic seismicity record. To do this the concepts of seismic moment and moment magnitude must be introduced. The seismic moment is the product of 3 parameters and can be defined as:

$$M_o = \quad ULW \tag{2}$$

where is the rigidity, U is the fault slip and LW is the product of the fault length and width, or the area of the rupture surface. Seismic moment is therefore directly proportional to both the amount of fault movement and the area of the rupture surface. It has also been shown that the slip is proportional to length of rupture such that,

$$U = \quad L \tag{3}$$

where is a constant of proportionality. As all the faults in the San Francisco Bay Area are of the strike slip type we may assume a constant fault width (depth) of 10 km. With a value of 1.1×10^{-5} for the constant of proportionality (Joyner and Fumal) and a value of 3.4×10^{11} dyne/cm for the rigidity we may substitute 3 into 2 to obtain

$$M_o = U^2 W/ \quad (4)$$

$$M_o = U^2 \times 3.091 \times 10^{22} \quad (5)$$

which relates seismic moment to fault-slip.

Moment magnitude as defined by Hanks and Kanamori (1979) is obtained from seismic moment by the relationship:

$$M = 0.67 \log M_o - 10.7 \quad (6)$$

As an example if we assume 100 cm. of slip in equation (5) the moment magnitude M is represented by equation (6) is 7.0. Estimates of the moment magnitude of the 1906 San Francisco earthquake (Thatcher, 1975) are between 7.7 and 7.8. It is now generally agreed that this represents the maximum value for a strike slip transform fault system such as the San Andreas. This is a significant limit and requires careful distinction in the study between the different magnitude scales. The magnitude of record for the 1906 San Francisco earthquake remains at 8.25 but the hazard study which uses moment magnitude has a limiting value of 7.75 for California.

The seismic moment accrual in the study zone per year using the geodetic slip rate of 6 cms should therefore be

for annual slip rate given by $\dot{\bar{u}}$

$$M_o = A\dot{\bar{u}} \quad (7)$$

$$= 3.4 \times 10^{11} \ (10 \times 240 \times 10^{10}) \ 6 \quad (8)$$

$$= 4.89 \times 10^{25} \text{ dyne cm/year} \quad (9)$$

This value represents a maximum value as some of the geodetic slip is relieved without earthquake development. This value can be used to show that if the total slip were relieved by only maximum sized events on the San Andreas fault, a hypothesis which is unacceptable, the recurrence interval for these large events would be at least 100 years. The consideration instead is to find the equivalent integrated slip which would be relieved within our study area by events distributed in size to satisfy the recurrence rate given by Figure 3.

The seismic activity can be represented in the computerized model in several ways. The procedure developed by Cornell (1968) has been extended by his coworkers and others to include source models with complex geometry and models with options perhaps more simply described as seismic memory. In most cases the analytical techniques are far more advanced than the quality of the data which can be used in them. For this reason we only use the more complex form of seismic model in situations where the data are of especially good quality and the source model is well understood.

The size of the source area was chosen so that the contribution to the overall seismic risk from activity outside the region is negligible. The seismic activity within the model can be represented as coming from areal, point, or line sources. The use of closely spaced point sources is the preferred analytical method because it is more efficient for computational purposes. The USGS open file program by McGuire reduces to a point-source representation before probability computation. Studies by Cornell and Vanmarcke (1969) showed that both area and line sources can be accurately approximated by point sources provided the point source spacing is carefully scaled. It is also possible with a point source model to represent curved faulting surfaces and to permit fault rupture propagation. The point source model for the San Francisco study was obtained by overlaying a grid on the detailed fault map summarized in Figure 1.

The seismic activity was distributed amongst the seismic sources in accordance with their anticipated activity. A small proportion of the total activity of modest earthquakes (moment magnitudes of less than 6) was assigned as a random areal distribution. The maximum magnitude on each fault was a function of its length in accordance with equations (2) through (6). Additionally to maintain consistency with the total seismicity the activity rates on individual faults were proportionally increased when other sources reach their magnitude limited. This requirement also anticipates that the maximum earthquake can only be produced by the San Andreas Fault. The activity distribution and the fault length limited upper magnitudes both require that at least two thirds of the accumulated tectonic slip in the San Francisco Bay Area be released by seismic activity along the San Andreas Fault.

The final major input requirement for the analysis is the assumption of an attenuation relationship that can relate the change in the desired ground motion parameter to the distance of the site from the source and to the size of the earthquake. Much more data on attenuation are available today than when I first attempted to apply probabilistic seismic hazard studies in design applications. There was interest in strong motion parameters but with few data there was no way to sift through the widely varying interpretations that had been published. The February 9, 1971 San Fernando Earthquake provided a large body of data and has since become perhaps the most widely investigated earthquake. It provided, with the strong motion records at Pacoima Dam which was at that time a new high in recorded peak acceleration values, an added impetus for the continuing study of the attenuation of ground motion with distance. Immediately after San Fernando several relationships appeared which were a combination of judgment and data. As a few subsequent data were gathered new relationships were developed which predicted higher and higher values. This process reached its peak in values described by Idriss (1978). The Imperial Valley and the Coyote Lake earthquakes of 1979 and the Livermore earthquakes of 1980 greatly extended the data base and forced a more moderate approach which led to a reduction of estimates from those obtained from many of the relationships developed prior to these events. There is now a reasonable consensus regarding attenuation of peak ground acceleration in California (Donovan, 1983).

A selection of recent peak acceleration attenuation equations is shown on Figure 4 for two different magnitude levels. The arithmetic scale used for the acceleration value allows direct gauging of the amplitude of equation variations rather than disguising them with a logarithmic scale. A representation of the average mean for several magnitudes is shown on Figure 5.

As more researchers entered the field it has also been possible to develop direct attenuation equations of spectral response values. McGuire (1974) first attempted to obtain spectral response attenuation equations. With the expanded data base Joyner and Boore (1982) developed spectral attenuation parameters. This work was extended to more closely represent site effects by Joyner and Fumal (1985) and it is these relationships which we have used in our recent San Francisco studies. The form of the Joyner and Fumal attenuation is as follows:

$$\log y = C_0 + C_1(M-6) + C_2(M-6)^2 + C_3 \log r + C_4 r + S \qquad (11)$$

$$5.0 \leq M \leq 7.7$$

$$r = (d^2 + h^2)^{1/2}$$

$S = 0$ at rock sites

$= C_5$ or equation (12) at soil sites

where y is the ground motion parameter to be predicted, M is moment magnitude (Hanks and Kanamori, 1979), and d is the closest distance in kilometers from the site where ground motion is being predicted to the vertical projection of the earthquake fault rupture on the surface of the earth. As the reference by Joyner and Fumal is part of a larger study that is not widely available the parameters for use in the equations for the mean horizontal component of pseudo-acceleration response (g) at 5 percent damping and of peak acceleration (g) and velocity (cm/s) are given here in Table 1. For use on soils with estimated shear wave velocities an alternate form of the site effect term is given. In place of the coefficient C_5 the alternate site effect term becomes

$$S = C_6 \log \left(\frac{V}{V_o}\right) \qquad (12)$$

where V is the local shear wave velocity and V_o is a reference velocity. Values of C_6 and V_o are given in Table 2 except for peak acceleration and a few of the short period response values for which the correlation of the ground motion and the shear wave velocity is not statistically significant.

Probabilistic response spectra for a section across the San Francisco area using an extension of the study area shown in Figure 1 was completed in preparation of another paper (Donovan and Becker, 1986). The probabilistic response spectra obtained for a downtown San Francisco soil profile site for several mean recurrence intervals are shown in Figure 6. The values of variance given by Joyner and Fumal (see Table 1) were used in the integration to obtain the spectral motion probabilities.

The most important point to make in the spectra shown on Figure 6 is the nonuniformity of shape between the spectra. This demonstrates that the commonly

used practice of scaling response spectra by using the probabilistic response acceleration and a constant spectral shape can yield results which are inconsistent.

For the cross-section of the San Francisco area shown on Figure 6 it is possible to show the variations in spectral parameters across the section. Sample values for several quantities are shown in Figure 7. These are mean peak accelerations determined directly from the attenuation equation, together with the probabilistically determined 500 year acceleration, the spectral acceleration at a 0.4 second period, and the spectral acceleration at a 1.5 second period. The locations of the individual fault crossings are easily identified on Figure 7 as occurring at the distances where local peak values occur.

The values of Figure 7 are shown normalized with respect to the maximum value at the San Andreas Fault crossing in Figure 8. The normalized results on Figure 8 allow several conclusions to be drawn. These may appear contradictory at first:

1) The attenuation of spectral values with distance from the principal faults is more rapid than the attenuation of the probabilistic peak acceleration.

2) The attenuation of the larger period spectral values is more rapid than short period spectral values.

3) The attenuation of peak acceleration estimated by attenuation equations using the maximum event on each fault is more rapid than the probability based peak acceleration.

The apparent contradiction to the generally accepted conclusions that long period quantities attenuate more slowly is not supported by the above conclusions. Each set of values in Figures 7 and 8, with the exception of the values identified as "mean attenuation relationship" is computed from a total probability which includes the contribution from all seismic sources. Because spectral values become more magnitude dependent as the period lengthens the contributions to the points more distant from the major faults become an increasingly smaller portion of the total probability at that point. The slow

attenuation of the probabilistic peak acceleration is a consequence of the same phenomenon. Peak acceleration is much less sensitive to magnitude than spectral values so when the probability is integrated, with the error estimates included, a large portion of the probability contribution comes from nearby events.

Although not shown on Figure 8 the profile of the velocity to acceleration ratio (v/a) also demonstrates the dominance of the distance from the large earthquakes as the v/a value. The v/a ratio has been shown to increase with magnitude and with distance. The probabilistic value of v/a across the profile decreases rapidly with increasing distance showing that the increase with magnitude overrides the anticipated v/a ratio increase with increasing distance. This is a further example which shows that determistic interpretations may be different and cannot be applied in probabilistic studies.

RESPONSE SPECTRA

The ATC3-06 code recommendations did not include direct recommendations for the development of response spectra. Response spectra are included in the tentative lateral force requirements of the Structural Engineers Association of California. These response spectra for the first 3 soil types are shown in Figure 9. As the spectra for Soil type 4 cover a wide range and cannot be represented by a single curve they are not included here.

The key ground motion parameters to be used with the spectral amplification value of 2.5 to develop the response spectra in the SEAOC guidlines are the velocity/acceleration (v/a) values of 24, 36 and 48 inches/sec/g for soil profiles 1, 2 and 3 respectively, and dimensionless parameter values (ad/v2) of 5 for soil profile 1, and 4 for the remaining soil profile types. It should be noted that the effects of distance and magnitude on response spectra shape both in deterministic studies and in probabilistic studies were not included in the recommendations for the proposed code.

The spectra shown on Figure 9 are close to those which would be obtained by using the 84th percentile spectral amplification values given by Newmark and Hall (1982).

The results of probabilistic studies that provide entirely risk based response spectra have tended to confirm that the choice of the median response is appropriate and still possesses a considerable degree of conservatism. Although it must be recognized that these wholly probabilistic spectra are only available for a few tectonic regimes they do demonstrate that the total risk at any site is the composite of both small and large events while the spectral development relationships developed without consideration of magnitude or distance have a bias towards spectra from large events.

Response Spectra for Different Probability Levels

There is an interest in possible modification of the ground motion level and the response spectral shape to represent the effect of the shorter assumed life of a strengthened building when compared to a new building. The direct effect of the shorter assumed life would be to reduce the effective peak acceleration value below the value represented on the seismic zone map. The response spectral shape will also change with the assumption of a decreasing lifetime. The major contribution to a probabilistic response spectra in the period range controlled by the ground velocity comes from high magnitude events. As large events have longer recurrence intervals than smaller events their contribution in the velocity controlled range will fall faster than the reduction in the maximum spectral acceleration. This effect is demonstrated in Figure 10 where the probabilistic response spectra for a range of mean recurrence intervals at a rock site are shown. The changing spectral shape and the more rapid decrease of the spectral values beyond a 0.3 second period as the recurrence interval is reduced are readily apparent.

A simple construction procedure that will accommodate the different recurrence interval is developed in this section. The effect of decreasing the assumed lifetime has been evaluated from the results of several specific site studies. The change in the values of these parameters may be expected to vary in different seismic regimes. For the purposes of general recommendations it is believed that average values of the parameters from a range of studies would be appropriate.

The peak acceleration values have been plotted against the estimated recurrence interval in years from several seismic hazard studies in Figure 11. These results which cover several states and territories have their numerical results changed so that all curves cross at 475 years, the recurrence interval equivalent to the 10 percent probability of exceedance in 50 years upon which the zoning map is based. The data shown on Figure 11 give an estimate of the approximate range of variation. Examination of the data in Figure 11 shows that the reduction in somewhat less where deep earthquakes occur. Over the range of greatest interest between 100 and 500 years the differences are small so the use of the mean relationship shown on the figure is the recommended approach. From the mean relationship a simple scaling relationship to compute values at different return periods was derived. This relationship can be used when different probabilities from those upon which the maps are based are required. This relationship is:

$$F = 0.18\ T_1^{0.28}$$

where F is the factor to multiply the map acceleration values by for different return periods T_1. The value of T_1 in years, appropriate for different probability levels can be obtained by assuming the Poisson distribution as follows. As an example, for a 20 percent probability of a exceedance in 50 years T_1 = (-50)/ln(1 - 0.2) or 224.1 years. Use of 224 years in equation 1 will give a value of 0.82 for F.

Figure 12 shows that the velocity to acceleration ratio (v/a) is a function of the recurrence interval. The spectra shown on Figure 10 are for a rock site. Similar spectra have been developed probabilistically for sites with soil profiles which has also allowed further examination of the variation of v/a ratio with recurrence interval. From this work a relationship for modification of the v/a ratio of 24, 36 and 48 inches/second/g used with 10 percent probability of exceedance in 50 years or T1 of 475 years have been developed. The relationship gives a scaling factor as follows:

$$F_{va} = -0.02 + 0.38 \log T_1$$

where T is the recurrence interval for the changed probability as described above. The data points used to derive equation 2 and the variation of v/a

represented by the equation are shown in Figure 12. For the same 20 percent in 50 year example the factor is 0.88 and the v/a ratio for spectral development of the soil site would be 0.88(36) or 31.7 in/sec/g.

Using the results given above spectra can be computed to represent reduced exceedance probability levels if consideration is given to the probably shorter lifetimes of existing buildings. The use of reduced probabilities could provide a means by which a local ordinance could be established which would allow a lesser level of compliance for non-critical structures in exchange for an agreed upon demolition date. Such a requirement would be on a one time only arrangement which could not be renewed.

Table 1

Attenuation Equation Parameters

Response spectra with 5 percent damping
after Joyner and Fumal (1985)

Period sec	C_0	C_1	C_2	h km	C_3	C_4 km-1	C_5	V_o m/sec	C_6	
0.1	0.97	0.25	-0.06	11.3	-1.0	-0.0073	-0.02			0.28
0.15	1.03	0.30	-0.08	10.8	-1.0	-0.0067	-0.02			0.28
0.2	0.97	0.35	-0.09	9.6	-1.0	-0.0063	-0.01			0.28
0.3	0.80	0.42	-0.11	6.9	-1.0	-0.0058	0.04	590	-0.28	0.28
0.4	0.64	0.47	-0.13	5.7	-1.0	-0.0054	0.10	830	-0.33	0.31
0.5	0.52	0.52	-0.14	5.1	-1.0	-0.0051	0.14	1020	-0.38	0.33
0.75	0.27	0.60	-0.16	4.8	-1.0	-0.0045	0.23	1410	-0.46	0.33
1.0	0.09	0.67	-0.17	4.7	-1.0	-0.0039	0.27	1580	-0.51	0.33
1.5	-0.18	0.74	-0.19	4.7	-1.0	-0.0026	0.31	1620	-0.59	0.33
2.0	-0.37	0.79	-0.20	4.7	-1.0	-0.0015	0.32	1620	-0.64	0.33
3.0	-0.65	0.85	-0.22	4.7	-0.98	0.0	0.32	1550	-0.72	0.33
4.0	-0.84	0.88	-0.24	4.7	-0.95	0.0	0.29	1450	-0.78	0.33
Peak Acceleration	0.43	0.23	0.0	8.0	-1.0	-0.0027	0.0			0.28
Peak Velocity	2.09	0.49	0.0	4.0	-1.0	-0.0026	0.17	1190	-0.45	0.33

All equations except peak velocity give acceleration or spectral acceleration in units of g. Peak velocity is given in cm/sec. Values represent mean of both horizontal components of motion. Note that variance is expressed as a base 10 logarithm.

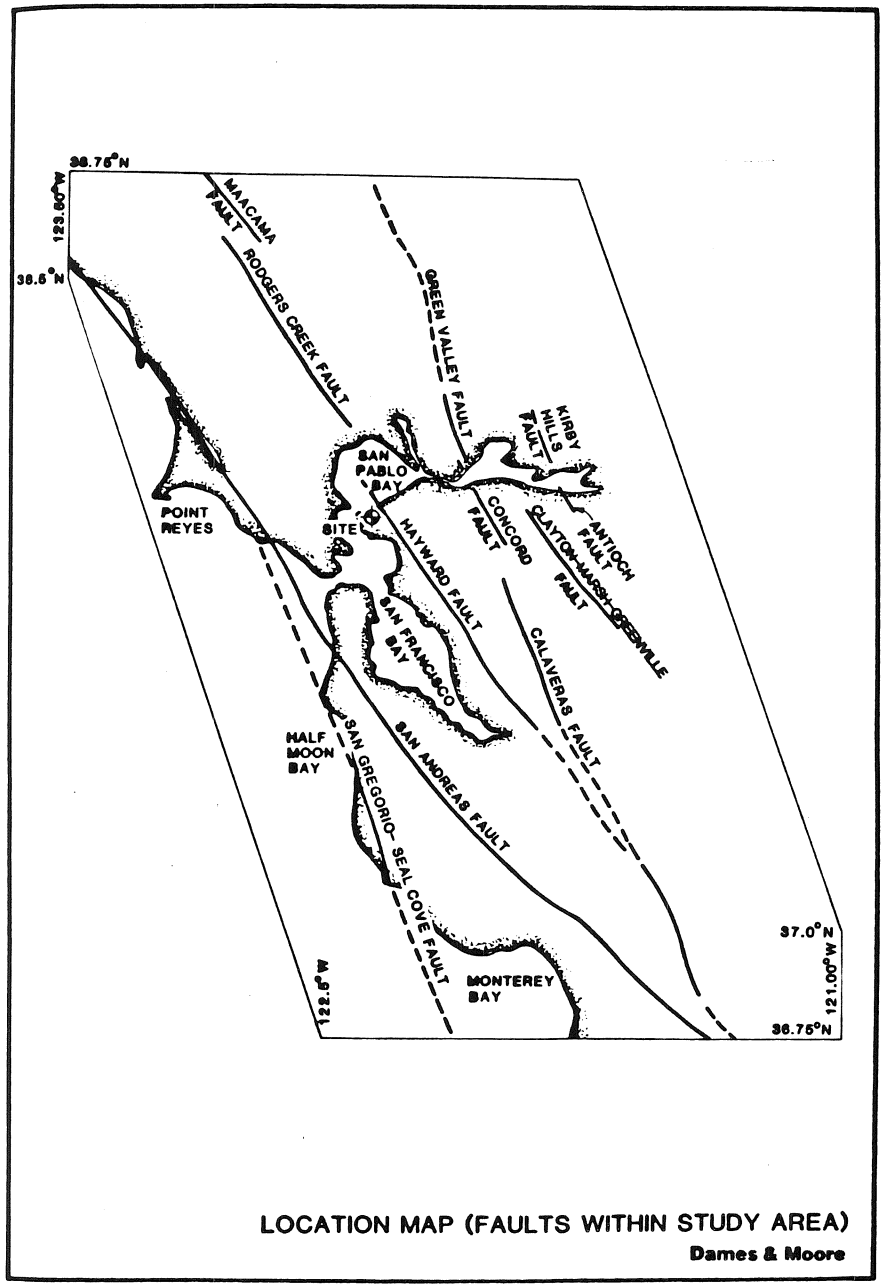

Figure 1

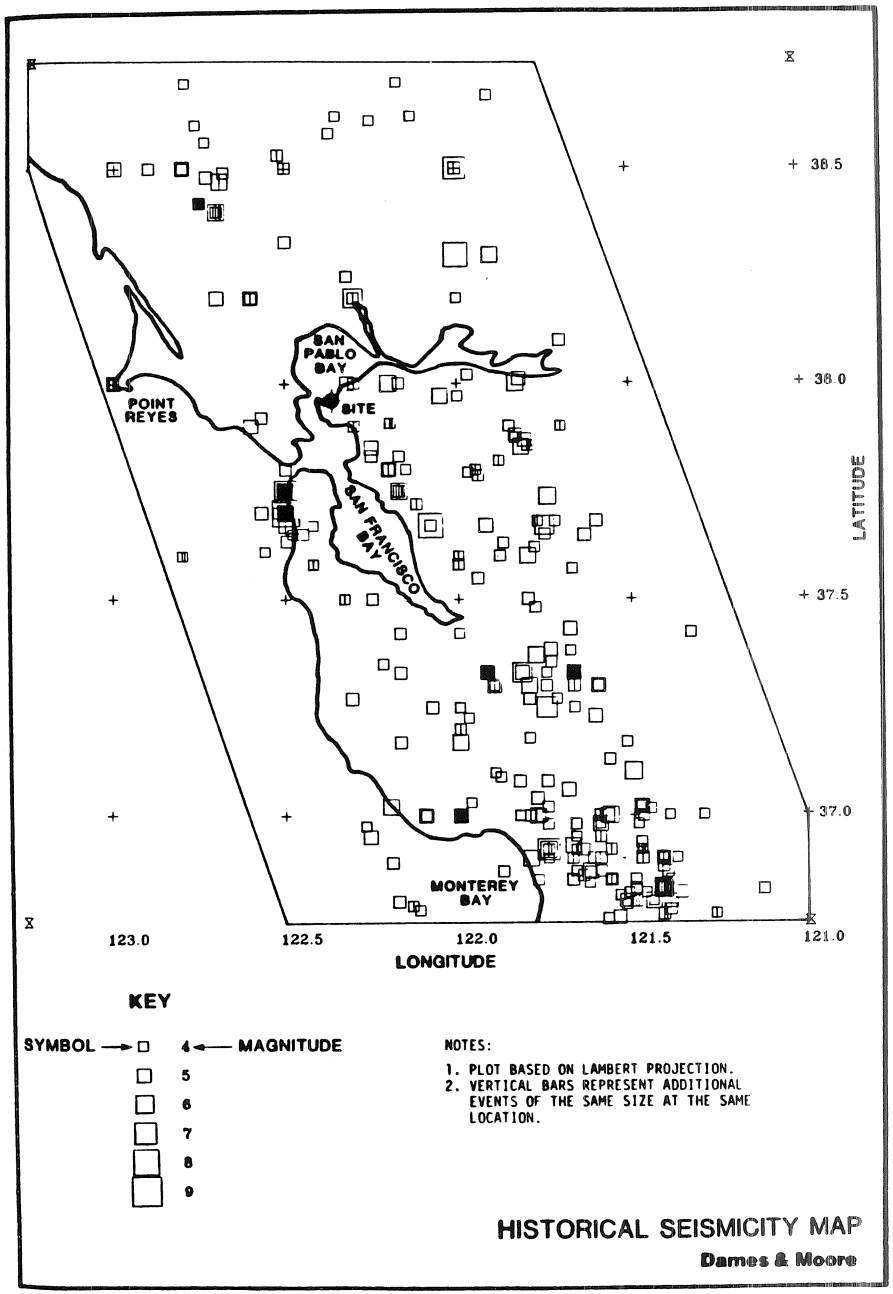

Figure 2

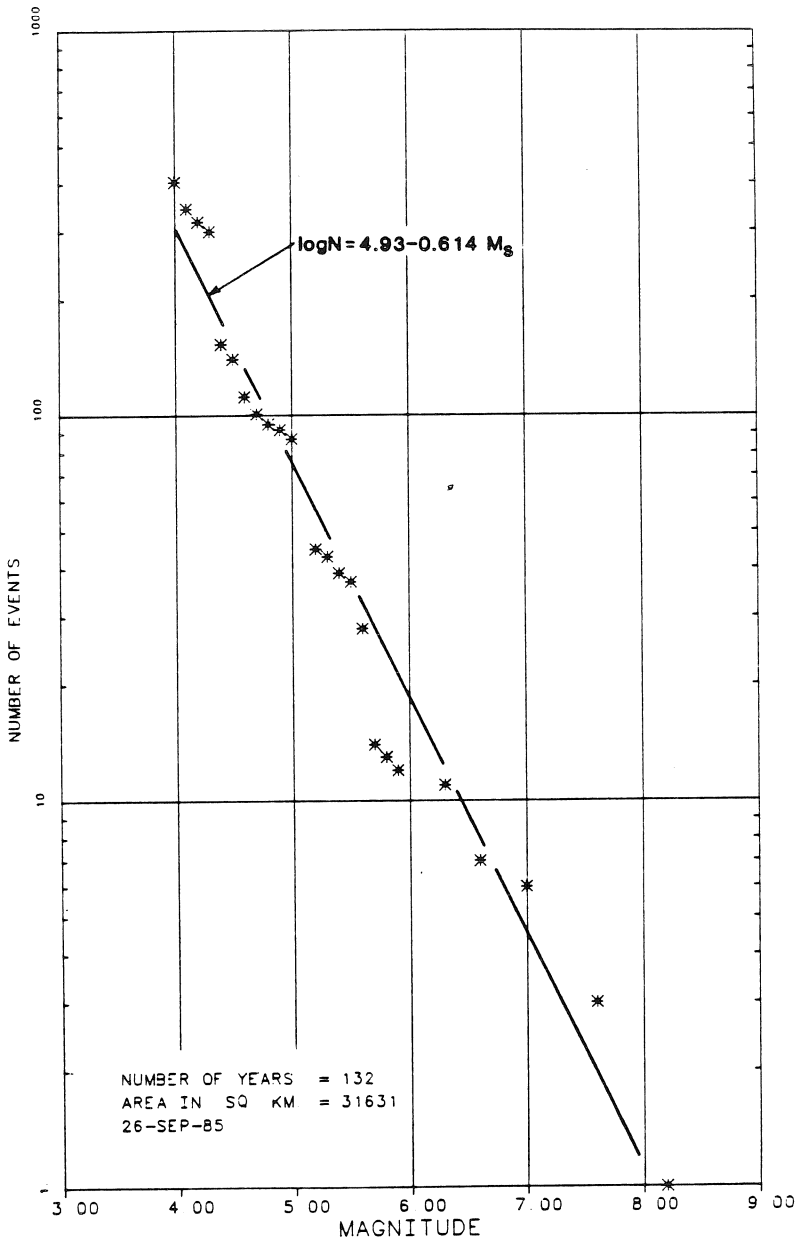

HISTORICAL SEISMIC ACTIVITY RATE

Dames & Moore

Figure 3

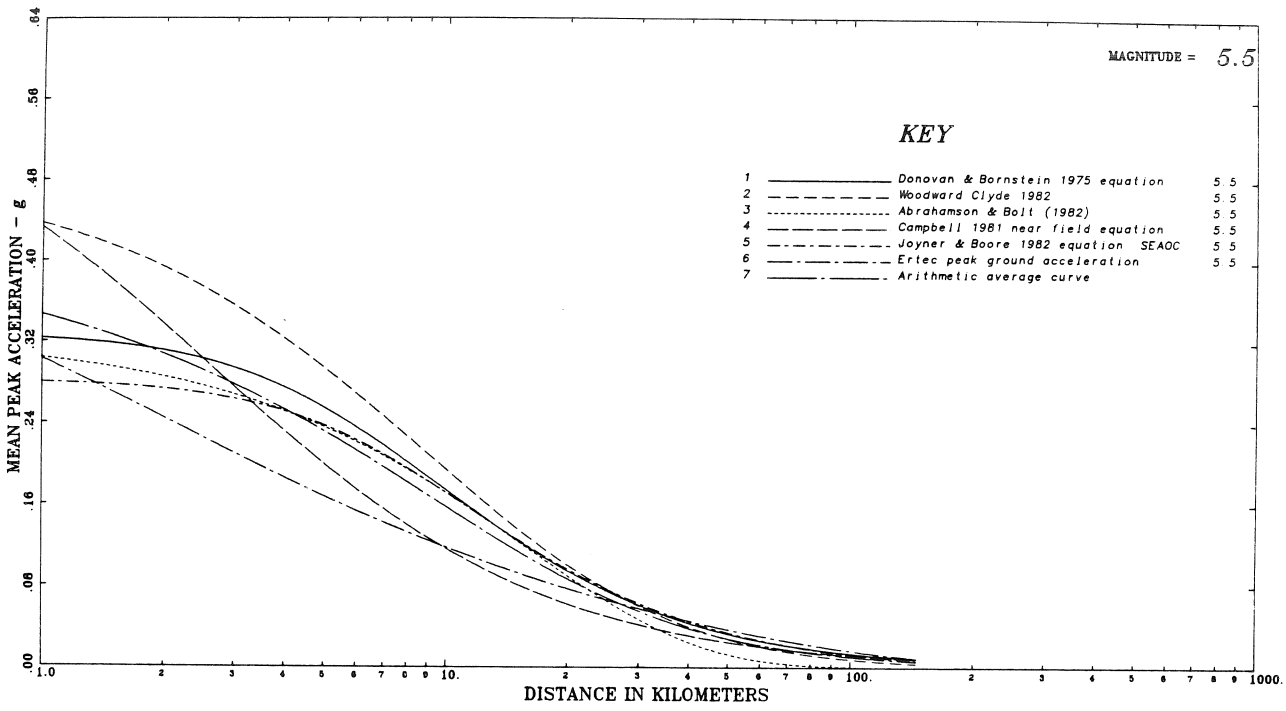
MAGNITUDE = 5.5
KEY
1 Donovan & Bornstein 1975 equation 5.5
2 Woodward Clyde 1982 5.5
3 Abrahamson & Bolt (1982) 5.5
4 Campbell 1981 near field equation 5.5
5 Joyner & Boore 1982 equation SEAOC 5.5
6 Ertec peak ground acceleration 5.5
7 Arithmetic average curve
MEAN PEAK ACCELERATION - g
.00 .08 .16 .24 .32 .40 .48 .56 .64
1.0 2 3 4 5 6 7 8 9 10. 2 3 4 5 6 7 8 9 100. 2 3 4 5 6 7 8 9 1000.
DISTANCE IN KILOMETERS

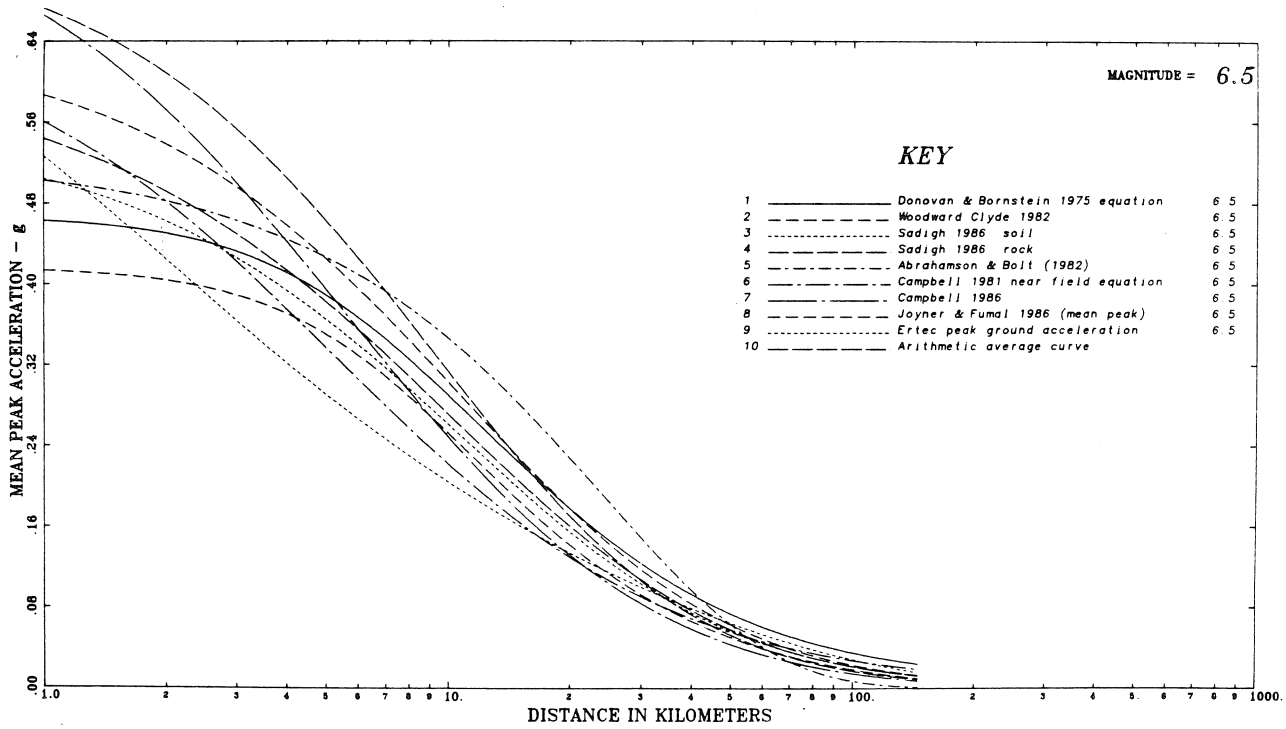
MAGNITUDE = 6.5
KEY
1 Donovan & Bornstein 1975 equation 6.5
2 Woodward Clyde 1982 6.5
3 Sadigh 1986 soil 6.5
4 Sadigh 1986 rock 6.5
5 Abrahamson & Bolt (1982) 6.5
6 Campbell 1981 near field equation 6.5
7 Campbell 1986 6.5
8 Joyner & Fumal 1986 (mean peak) 6.5
9 Ertec peak ground acceleration 6.5
10 Arithmetic average curve
MEAN PEAK ACCELERATION - g
.00 .08 .16 .24 .32 .40 .48 .56 .64
1.0 2 3 4 5 6 7 8 9 10. 2 3 4 5 6 7 8 9 100. 2 3 4 5 6 7 8 9 1000.
DISTANCE IN KILOMETERS

Figure 4

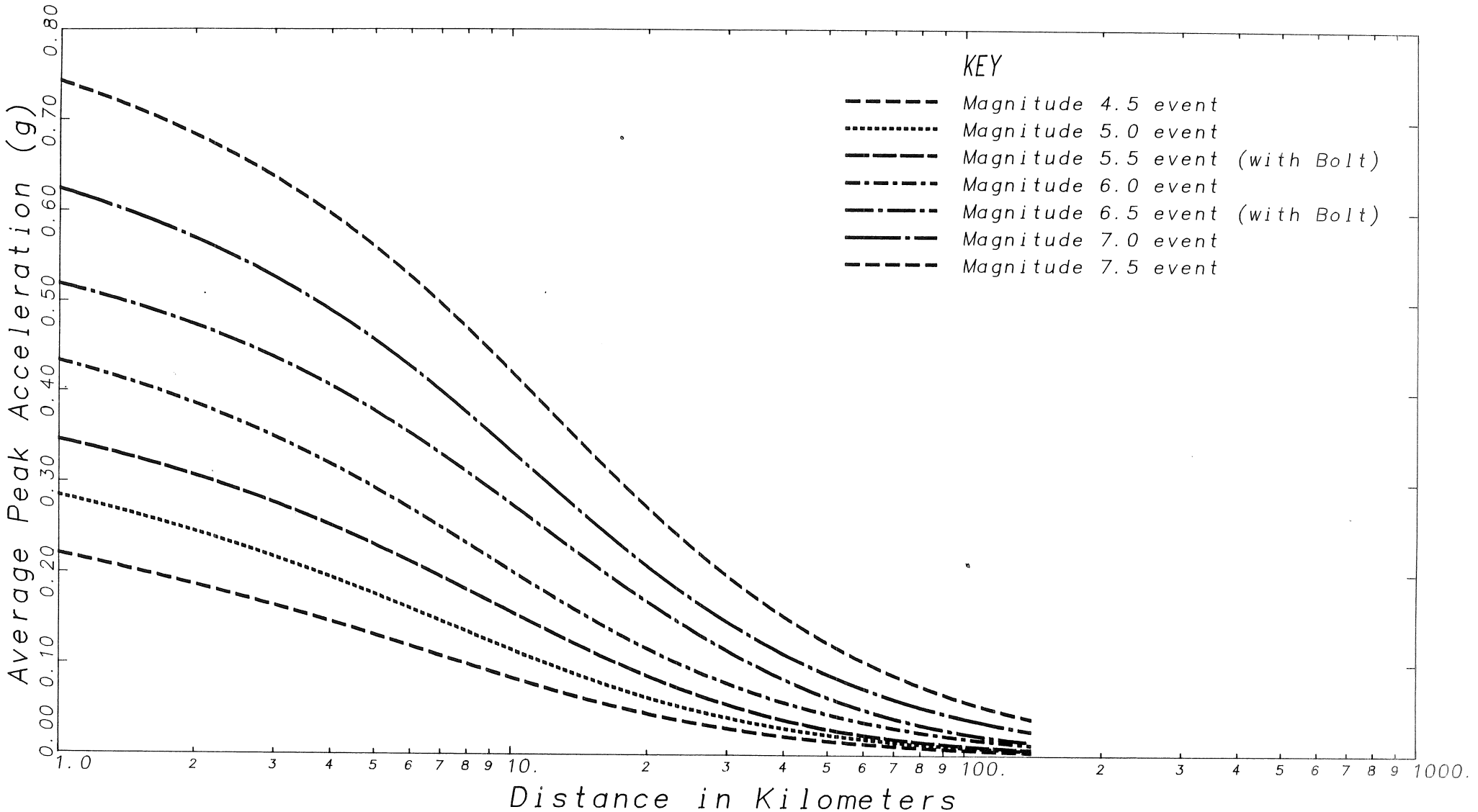

Acceleration attenuation relationship average curves (November 13, 1986) Based on equations by Bolt, Campbell, Donovan, Ertec, Joyner & Fumal, & Woodward Clyde

Figure 5

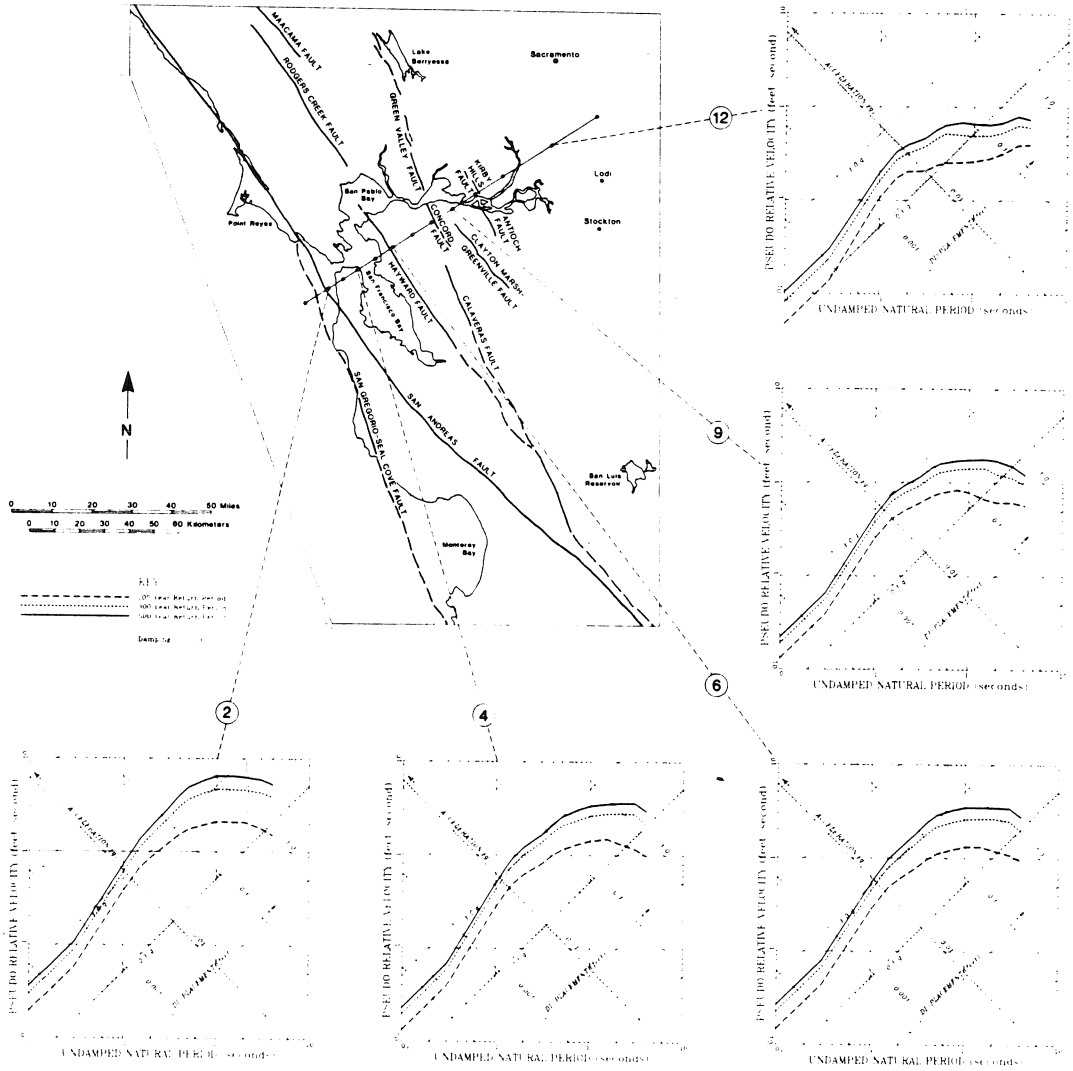

SAN FRANCISCO BAY FAULTS. RISK MODEL SECTION ACROSS ACTIVE REGION WITH SAMPLES OF HAZARD ANALYSIS RESPONSE SPECTRA.

Figure 6

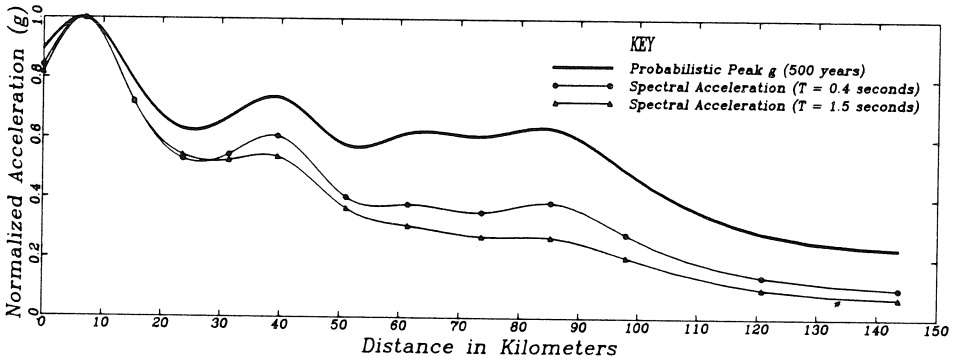

Comparison Between Peak Acceleration and Spectral Acceleration

Figure 7

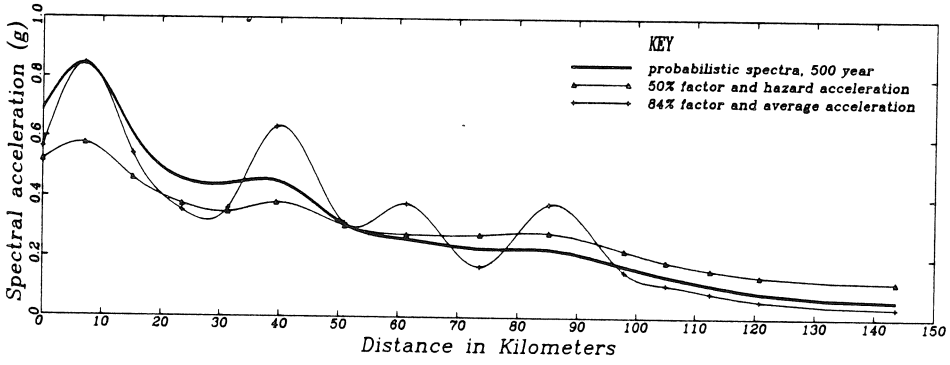

Variation of the Spectral Acceleration at a 1.5 Second Period Using Alternative Spectral Constructions

Figure 8

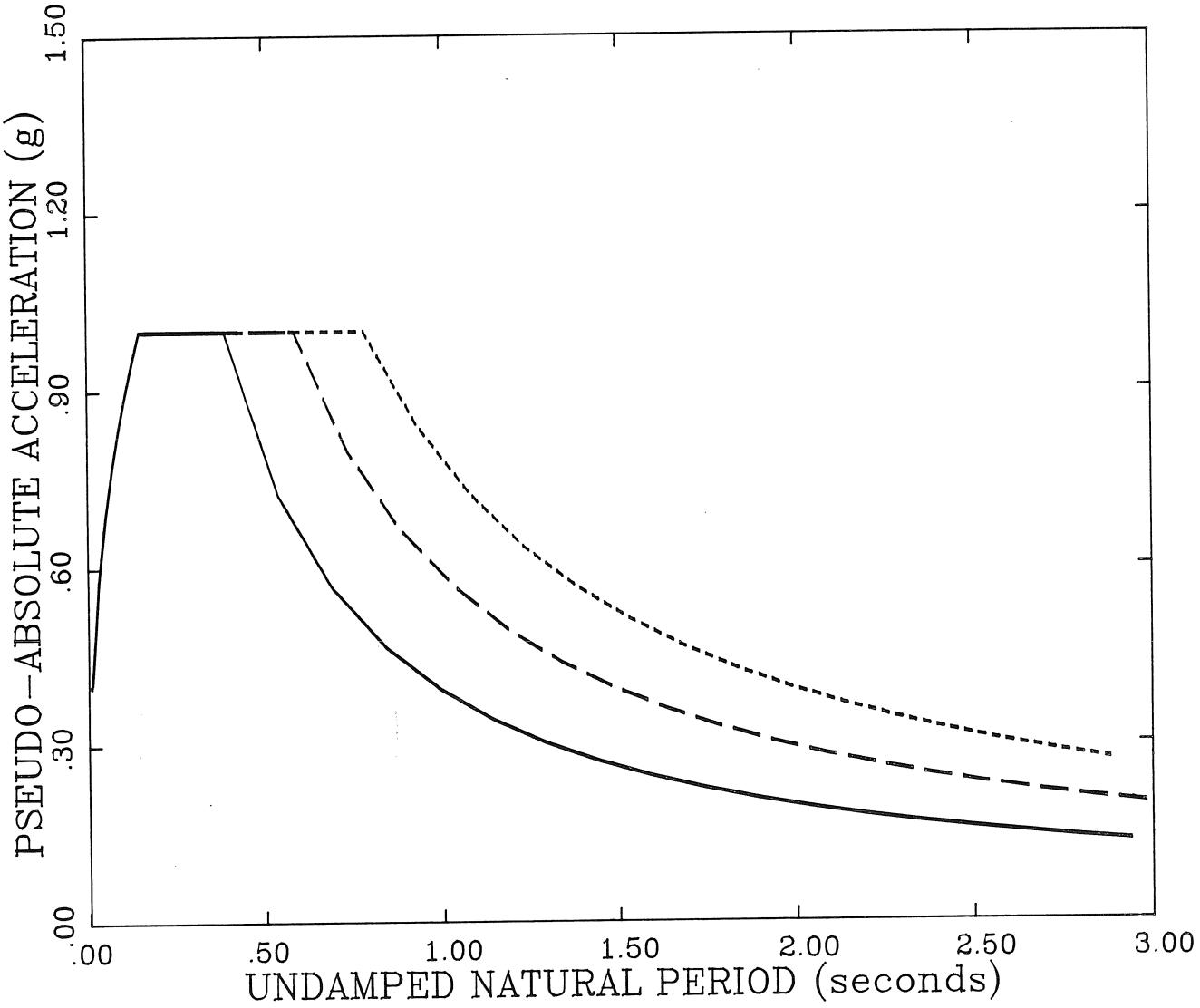

Seismic Zone 4. RESPONSE SPECTRA

Damping = 5.0

Figure 9

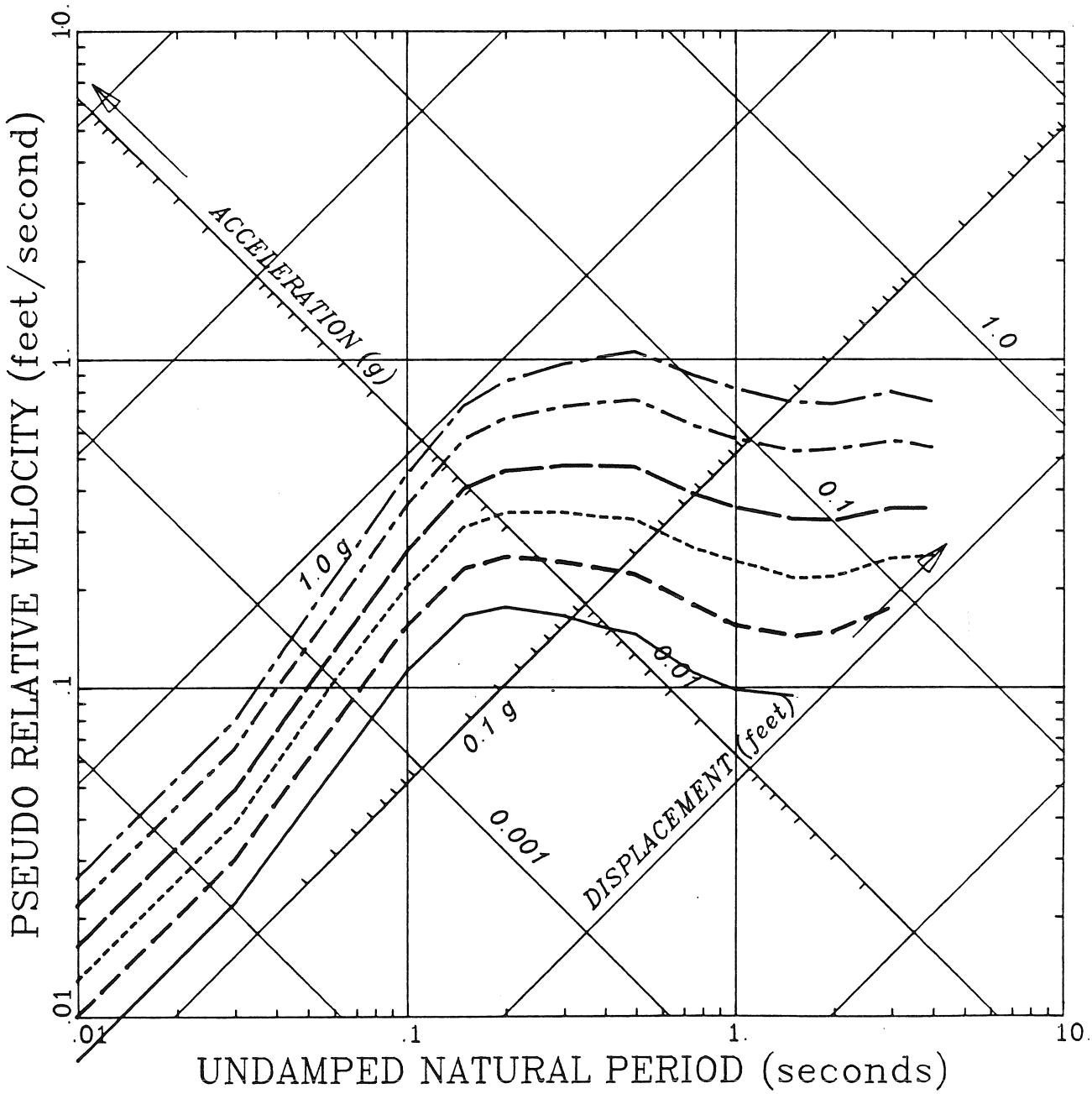

Risk Based Spectra at a Rock Site with Different Return Periods

Damping = 5.0

Figure 10

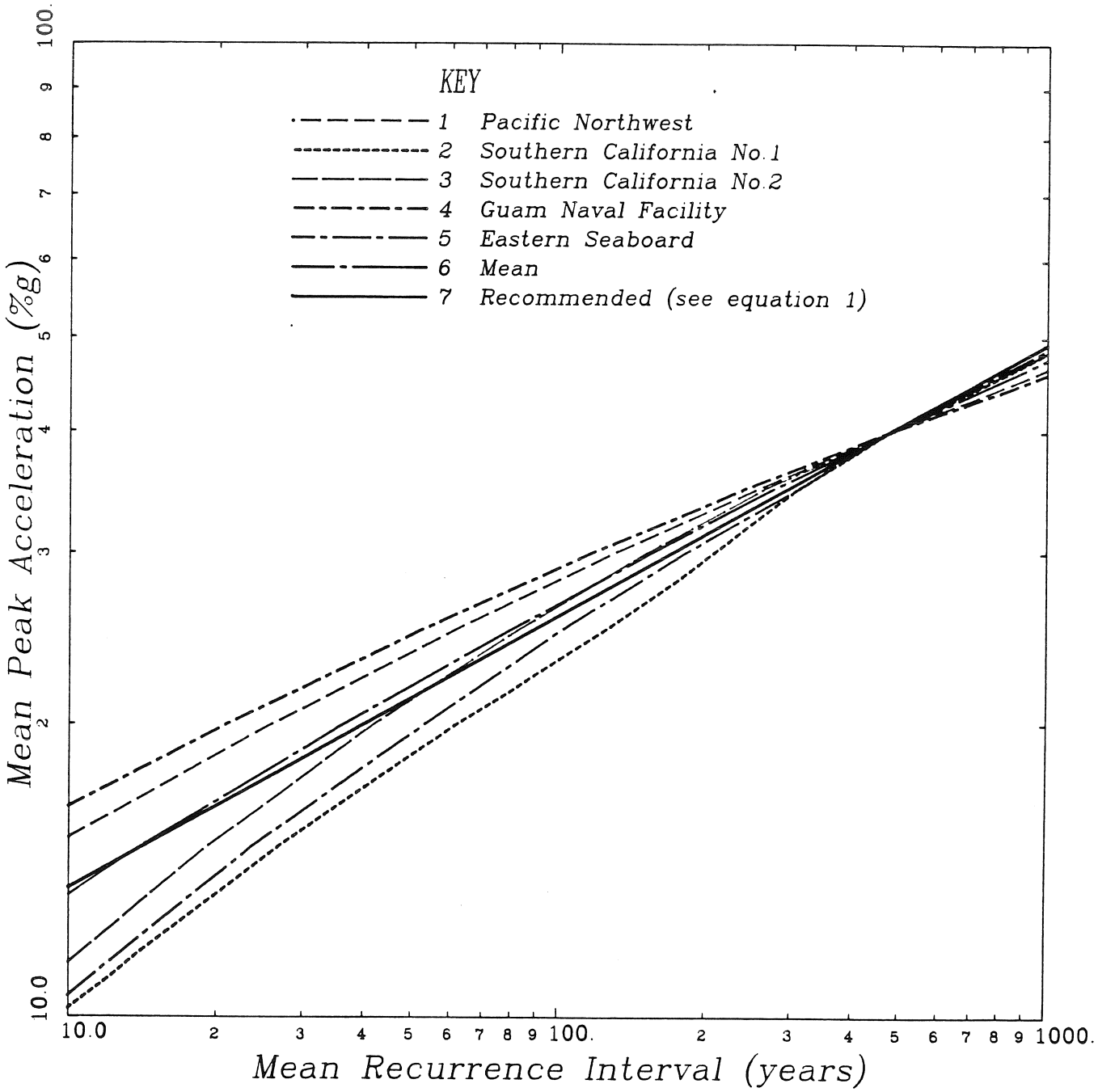

Examples of Recurrence Interval Variations Used to Obtain the Recommended Equation. All Curves scaled to give the same value at 475 years.

Figure 11

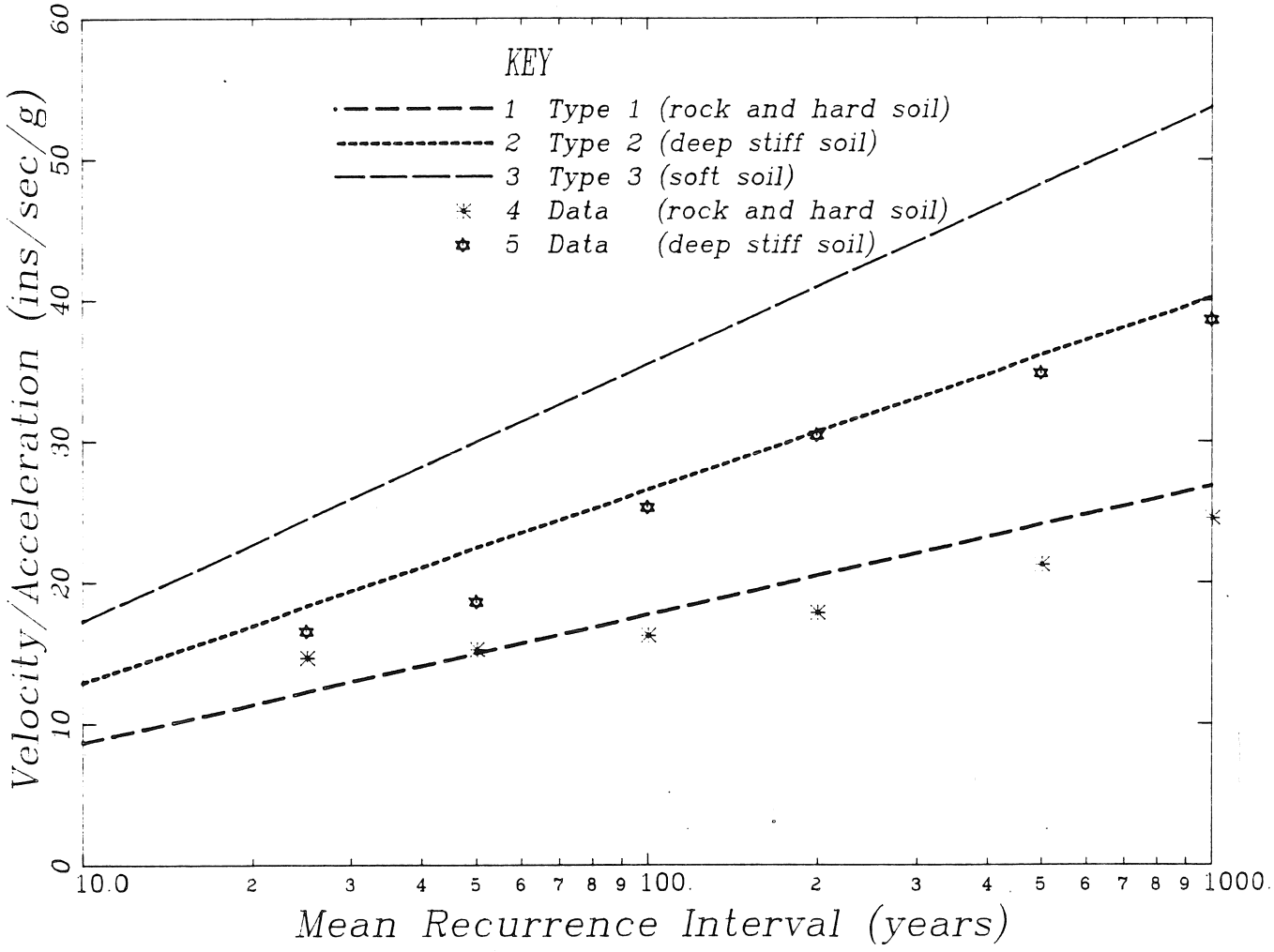

Recommended Variation of (v/a) Ratio for Changing Recurrence Intervals. Values at 475 Years Are Consistent With Basic Guidelines

Figure 12

APPENDIX

SIMPLIFIED SPECTRAL CONSTRUCTION PROCEDURES

Preferred Method

This method requires the results of a probabilistic hazard analysis for peak acceleration. These can be obtained from probabilistic based hazard maps. Because there is an increasing interest in the use of this type of map for code use, they are becoming more available. The results shown above for the San Francisco Bay profile compare well with values obtained from the map given as Figure C1-3 in the ATC3-06 [2] report except in the zone close to fault crossings. The developers of the map specifically excluded use of the map close to fault crossings.

Step 1: Select the peak acceleration value for the appropriate probability (return period) for the project site.

Step 2: Using Eq. 1 compute the v/a ratio for the event which would be expected to control the deterministic approach to the design. This is usually the maximum event on the closest fault to the project site. Note that the v/a ratio is dependent on the site soil profile type. Compute the appropriate velocity using the acceleration obtained in step 1.

Step 3: Compute the maximum relative ground displacement from the dimensionless ad/v^2 term. This term may be given the value of 5 for rock sites and 4 for soil sites.

Step 4: Use the equations given by Newmark and Hall [9], included here as Table 1, to compute the median values for spectral amplification factors to be used with the values of acceleration, velocity, and displacement.

Table 1 Equations for Spectral Amplification Factors for Horizontal Motion (from Newmark and Hall [9])

Quantity	Cumulative Probability %	Equation
acceleration	50 (median)	3.21 - 0.68ln(b)
velocity		2.31 - 0.41ln(b)
displacement		1.82 - 0.27ln(b)
acceleration	84.1 (one sigma)	4.38 - 1.04ln(b)
velocity		3.38 - 0.67ln(b)
displacement		2.73 - 0.45ln(b)

where b is the damping ration expressed as a percentage of critical damping

Step 5: Construct the desired response spectra on a tripartite format using the values obtained in step 4 together with the peak acceleration. A description of the construction procedure is given in Newmark and Hall [9].

Alternate Method

This procedure may be used to approximate the design response spectra when the results of a probabilistic analysis or hazard maps are not available. This method is shown for convenience and should only be used for non-critical structures or when the other methods cannot be implemented. The large perturbations of the peak acceleration values along the profile shown on Fig. 3 are obtained from direct use of the attenuation equations. These can result in overestimation of spectral requirements close to a fault and possible underestimation of requirements elsewhere.

Step 1: Using an appropriate attenuation equation select the peak acceleration given by the maximum event on the fault closest to the site. The average attenuation curves given in the appendix could be used.

Step 2: Using Eq. 1 compute the v/a ratio for the event which would be expected to control the deterministic approach to the design. This will be the same event as used in step 1. Note that the v/a ratio is dependent on the site soil profile. Compute the appropriate velocity using the acceleration obtained in step 1.

Step 3: Compute the maximum relative ground displacement from the dimensionless ad/v^2 term. This term may be given the value of 5 for rock sites and 4 for soil sites.

Step 4: Use the equations given by Newmark and Hall [9] in Table 1 to compute the 84th percentile values for the spectral amplification factors to be used with the values of acceleration, velocity, and displacement.

Step 5: Construct the desired response spectra on a tripartite format using the values obtained in step 4 together with the peak acceleration.

$$\log (v/a) = 0.92 + 0.065\ M + 0.00127\ R + 0.23\ S \qquad (1)$$

where $R^2 = d^2 + 7.5^2$

$S = 1$ for soil

$= 0$ for rock

and M is moment magnitude, and d is the shortest distance to the surface projection of the aftershock area. The v/a ratio is given in inches/second/g when distances in kilometers are used.

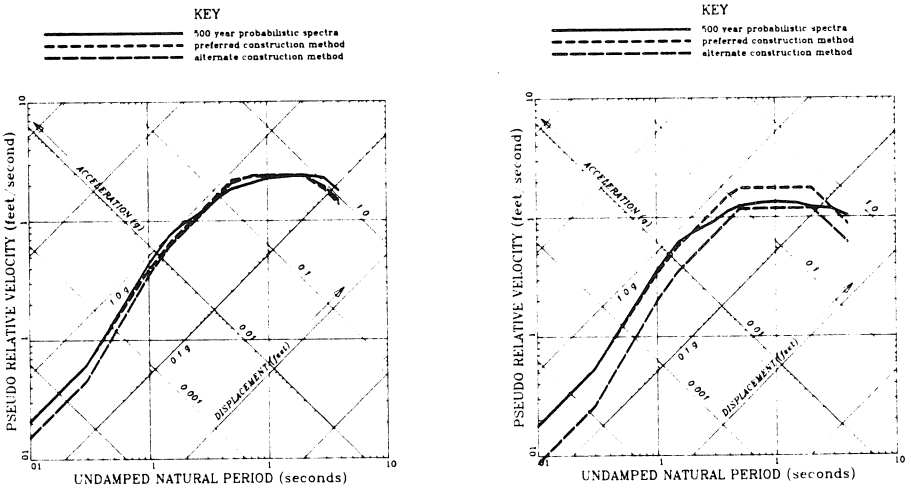

Hazard Analysis and Constructed Spectra - 50 (Left) and 100 (Right) Kilometers Along Cross-Section